© 2025. Published by The Company of Biologists | Journal of Experimental Biology (2025) 228, jeb249607. doi:10.1242/jeb.249607

RESEARCH ARTICLE

The key to bubble-net feeding: how humpback whale morphology functionally differs from other baleen whales

Cameron Nemeth[1,*], William T. Gough[1,2], Paolo S. Segre[2,3], Frank E. Fish[4], Andrew Szabo[1,5], Wesley N. Fassmann[6], Scott L. Thomson[6,7], Martin van Aswegen[1,5], Julia A. Burrows[8,9], Ellen M. Chenoweth[10], Jacopo di Clemente[11,12], Ari S. Friedlaender[13], Jeremy A. Goldbogen[2], Malene Simon[14], Janice M. Straley[15], Simone K. A. Videsen[12,16], Fleur Visser[17,18], Caroline R. Weir[19] and Lars Bejder[1,16]

ABSTRACT

Maneuverability in cetaceans is facilitated by pectoral flippers, flukes and spinal flexibility, features that are pronounced in humpback whales (*Megaptera novaeangliae*). Humpback whales exhibit several foraging tactics requiring high maneuverability not seen in other baleen whales, including bubble-net feeding. We hypothesized that the significant lift force produced by the humpback whale's uniquely large pectoral flippers will result in them being the only species observed executing the tight, high-speed, sustained turns characteristic of solitary bubble-net feeding. To test this hypothesis, we used a combination of inertial sensor tag data and unoccupied aerial systems (UAS; drone) photogrammetry to quantify the turning performance of solitary bubble-net feeding humpback whales, and compared this to similar data from six other mysticete species. We found that solitary bubble-net feeding humpback whales exhibited centripetal accelerations (0.46 m s^{-2}) that exceeded the upper limit quantified in comparable turns by all six other mysticetes. This enhanced turning performance can be attributed to a substantial lift force generated by the humpback whale's pectoral flippers (7800±85 N), which contributes to centripetal acceleration and facilitates faster roll rates, allowing humpback whales to more quickly bank inwards and utilize their spinal flexibility to decrease their turning radius. Our findings demonstrate how humpback whales are uniquely adapted to exploit prey patches that might otherwise be insufficient for capture by animals of such a large size.

[1]Marine Mammal Research Program, Hawai'i Institute of Marine Biology, University of Hawai'i at Mānoa, Kāne'ohe, HI 96744, USA. [2]Hopkins Marine Station, Stanford University, Pacific Grove, CA 93950, USA. [3]Department of Natural and Applied Sciences, University of Wisconsin, Green Bay, WI 54311, USA. [4]Department of Biology, West Chester University, West Chester, PA 19383, USA. [5]Alaska Whale Foundation, Petersburg, PO Box 1927, AK 99833, USA. [6]Department of Mechanical Engineering, Brigham Young University, Provo, UT 84602, USA. [7]Department of Mechanical and Civil Engineering, Brigham Young University-Idaho, Rexburg, ID 83460, USA. [8]Stanford University, Stanford, CA 94305, USA. [9]Division of Marine Science and Conservation, Duke University Marine Laboratory, Beaufort, NC 28516, USA. [10]College of Fisheries and Ocean Sciences, University of Alaska Fairbanks, Sitka, AK 99835, USA. [11]Department of Biology, University of Copenhagen, 2100, København Ø, Denmark. [12]Marine Mammal Research, Department of Ecoscience, Aarhus University, 4000, Roskilde, Denmark. [13]Ocean Sciences Department and Institute for Marine Sciences, University of California Santa Cruz, Santa Cruz, CA 95064, USA. [14]Greenland Climate Research Centre, Greenland Institute of Natural Resources, 3900 Nuuk, Greenland. [15]University of Alaska Southeast, Sitka, AK 99835, USA. [16]Zoophysiology, Department of Bioscience, Aarhus University, Aarhus 8000, Denmark. [17]Kelp Marine Research, 1624 CJ Hoorn, The Netherlands. [18]Department of Coastal Systems, Royal Netherlands Institute for Sea Research, Texel, 1790 AB Den Burg, The Netherlands. [19]Falklands Conservation, Stanley FIQQ 1ZZ, Falkland Islands.

*Author for correspondence (ncnemeth@hawaii.edu)

C.N., 0009-0009-1838-7059; P.S.S., 0000-0002-2396-2670

Received 25 September 2024; Accepted 15 June 2025

ADDITIONAL LANGUAGE ABSTRACT

Kōkua ʻia ka huli ʻana o nā cetaceans e ka ʻēheu, hiʻu a me ka palupalu o ka iwikuamoʻo, ahuwale nō kēia mau mea i ke koholā (*Megaptera novaeangliae*). Hōʻike ke koholā i nā ʻano alualu like ʻole he nui e koi ana i ka huli maikaʻi ʻana i ʻike ʻole i nā ʻano koholā aʻe, e like me ke alualu ʻupena huʻa. Ua manaʻo mākou, ma muli o ka huʻe aʻe o ka ikaika nui na nā ʻēheu nui laha ʻole o ke koholā; ʻaʻohe lua e like ai me ia hana. Pēnei nō i nā huli liʻi, ʻāwīwī, a wā lōʻihi i laha ma ke alualu ʻupena huʻa ponoʻī. I mea e hōʻoia ai i kēia manaʻo, hoʻohana mākou i ka mea paʻa ʻike a me ka paʻi kiʻi ʻana o ka helekopa uila liʻi (UAS) i helu i ka maikaʻi o ka huli ʻana o nā koholā pākahi e alualu ʻupena huʻa ana, a hoʻohālikelike ʻia me ka ʻike like o ʻeono mau ʻano koholā. ʻOi aku ka hoʻohikiwawe poepoe o ke koholā (0.46 m s^{-2}) ma mua o ke kōkī i helu `ia no nā huli like o nā ʻano koholā like ʻole. Ma muli nō o ka ikaika aʻe o ko ke koholā mau ʻēheu (7800±85 N) ka maikaʻi o ka huli ʻana, nāna e hoʻonui i ka hoʻohikiwawe poepoe a kōkua i ka wili wiki ʻana i mea e pelu ai i loko o ka pōʻai a hoʻohana i ka palupalu o ka iwikuamoʻo i hoʻoiki i kā lākou kahahānai. Kuhikuhi kā mākou ʻike mai kēia papahana noiʻi i kēia hua: maʻa kū kahi ke koholā i ke alualu ʻana i nā kula iʻa i lawa ʻole paha no ka hopu ʻia ʻana e kekahi holoholona nui loa.

KEY WORDS: Kinematics, Maneuverability, Foraging, Adaptation, Flipper, Baleen whales

INTRODUCTION

Cetaceans have evolved specialized morphologies allowing them to thrive in a variety of aquatic environments. Such morphological adaptations are fundamental to these species, enabling them to effectively forage (Goldbogen et al., 2017; Werth, 2007), dive (Snyder, 1983; Noren and Williams, 2000), travel (Fish, 2002), evade predators (Ford and Reeves, 2008; Howland, 1974) and rest (Fish et al., 2002). For example, the vertebral columns of dolphins are adapted to control body flexion and store elastic energy, enhancing propulsion while swimming (Long et al., 1997). Baleen whales (mysticetes) have evolved large engulfment capacities to maximize energetic intake (Goldbogen et al., 2017; Kahane-Rapport and Goldbogen, 2018; Videsen et al., 2023), and a low surface area to volume ratio that minimizes heat loss to the environment and reduces drag (Fish, 1993; Glarou et al., 2025; Noren and Rosen, 2023). Cetaceans spend all their lives in water, thus control surfaces are foundational morphological adaptations that shape their scope of movement and behavior in this medium (Fish, 2002; Weber et al., 2014). Control surfaces include the flukes, pectoral flippers and dorsal fin (Fish, 2002; Weber et al., 2014). Flukes are the primary morphological adaptation generating propulsive force in cetaceans (Fish and Hui, 1991), but are also associated with mobile joints, allowing an animal to twist their

flukes to initiate a change in orientation (Fish, 2002). Cetacean dorsal fins function to prevent side-slip and are typically highly swept in faster species (Fish, 2002; Fish and Rohr, 1999). Pectoral flippers are the most versatile of all control surfaces, aiding in both stability and controlled instability (Edel and Winn, 1978; Weber et al., 2014). Specialized control surface morphology is evident in baleen whales, with certain morphologies suited for stable high speeds and others favoring instability for low-speed maneuvering (Weber et al., 2014; Woodward et al., 2006). Control surface morphology is crucial in baleen whales for efficient foraging, as they must maneuver to target huge quantities of small prey to sustain their gigantic body size (Friedlaender et al., 2017; Goldbogen and Madsen, 2018; Segre et al., 2022).

One species in particular, the humpback whale (*Megaptera novaeangliae*), has a unique morphology distinguished by large flukes and pectoral flippers, the latter of which are approximately a third of their total body length (Clapham and Mead, 1999; Fish and Battle, 1995; Woodward et al., 2006). The considerable size of the humpback whale's pectoral flippers enhances maneuverability (Fish and Battle, 1995), enabling prey capture on a wide variety of prey types using various agile foraging tactics (e.g. Cade et al., 2020, 2022; Jurasz and Jurasz, 1979; Kosma et al., 2019; Weinrich et al., 1992). Some of these tactics, such as lunge feeding, require speed and/or a large engulfment capacity, and are similar to those adopted by other baleen whales (Acevedo et al., 2011; Kahane–Rapport and Goldbogen, 2018; Watkins and Schevill, 1979). Other tactics, such as inside-loop turns, tail slaps and bubble-net feeding, require high maneuverability (e.g. Jurasz and Jurasz, 1979; McMillan et al., 2019; Szabo et al., 2024; Wiley et al., 2011).

Bubble-net feeding has been documented in humpback whale populations worldwide, including in British Columbia, Southeast Alaska, the Gulf of Maine, the Australian coast and around the West Antarctic Peninsula, yet remains undocumented in other baleen whales (Allen et al., 2024; Cade et al., 2022; Clapham, 1996; Mastick et al., 2022; Pirotta et al., 2021; Szabo et al., 2024; Wray et al., 2021). Bubble-net feeding involves the formation of one or more discrete bubble 'rings' used to corral and concentrate prey (e.g. fish, krill), followed by a lunge up through the middle of the net to engulf the trapped prey (Wiley et al., 2011; Jurasz and Jurasz, 1979; Pirotta et al., 2021; Szabo et al., 2024). Other cetaceans have been documented utilizing various bubbling behaviors; for example, killer whales (*Orcinus orca*) blow bubbles to clear ice during coordinated attacks on seals resting on ice floes (Visser et al., 2008), gray whales (*Eschrichtius robustus*) blow bubbles to regulate their buoyancy during foraging (Bird et al., 2024) and Bryde's whales (*Balaenoptera edeni*) and fin whales (*Balaenoptera physalus*) produce bubble curtains (i.e. streams) associated with feeding (Kot et al., 2014; Ryan and Malcolm, 2022). However, humpback whales remain the only species to create this complex bubble ring structure that relies on a high degree of maneuverability.

Bubble-net feeding likely aggregates prey and prevents their escape by trapping them against the surrounding bubbles and the water surface, enabling humpback whales to increase their lunge efficiency (Allen et al., 2024; Sharpe and Dill, 1997; Szabo et al., 2024; Wiley et al., 2011). As baleen whales rely on a substantial amount of small-bodied prey to support their gigantic body sizes, targeting dense aggregations of prey is critical in maximizing foraging efficiency and individual fitness (Burrows et al., 2016; Goldbogen et al., 2011, 2015; Hazen et al., 2015). In Alaska, humpback whales feed on various small schooling fish and zooplankton. They bubble-net feed solitarily on krill (Fournet et al., 2018; Szabo et al., 2024), juvenile salmon (Kosma et al., 2019; Chenoweth et al., 2021) and Pacific herring (*Clupea pallasii*) (Fournet et al. 2018). When feeding on herring, a group of two or more whales can share a single bubble-net (Fournet et al. 2018). The largest group observed cooperatively bubble-net feeding on herring was 33 humpback whales recorded in Southeast Alaska (Shane Moore, pers. commun.). Solitary bubble-net feeding humpback whales in Alaska create bubble-nets composed of nested, internally tangential rings (Szabo et al., 2024). These whales actively control the number and size of rings in each net, with the final, innermost ring being seven times smaller than the outermost ring and only twice their gape size (Szabo et al., 2024).

Solitary bubble-net feeding requires a high degree of maneuverability to create these small, internally tangential rings (Fish and Battle, 1995), with pectoral flippers, flukes and spinal flexibility playing an important role in optimizing turning performance (Fish and Battle, 1995; Segre et al., 2019; Weber et al., 2014). The large planform area and high aspect ratio (i.e. span^2 planar area^{-1}) of the pectoral flipper generates maximum lift while minimizing drag (Fish and Battle, 1995; Fish et al., 2014; Goldbogen et al., 2017; Webb and De Buffrenil, 1990), facilitating higher rolling rates (Weihs, 1993) and allowing humpback whales to quickly bank inwards and utilize their spinal flexibility to minimize turn radius (Segre et al., 2019). Rolling also permits a greater planar area of the flippers to be directed toward the center of the turn, vectoring a greater percentage of the lift to increase centripetal acceleration (Fish, 2004; Fish and Battle, 1995). In addition to the large size of their pectoral flippers, tubercles (i.e. bumps) on the leading edge of the pectoral flippers function to maximize lift and prevent stall at high angles of attack (the angle between the flipper and the oncoming water flow) (Fish and Battle, 1995; Miklosovic et al., 2004; Weber et al., 2014), enhancing maneuvering performance as a control surface (Fish and Lauder, 2017). To achieve a smaller turning radius, many delphinids use unpowered turns in which the fluke and peduncle are disengaged from any propulsion, thus limiting speed and acceleration out of the turn (Fish, 2002). The large pectoral flippers of the humpback whale may allow for the completion of tighter turns without completely halting propulsive force production, which would maximize both speed and maneuverability, ideal for bubble-net feeding.

Prior work relating the large size of the humpback whale flipper with their turning performance has relied on lab-based modeling, rather than empirical data from free-swimming animals (Fish and Battle, 1995; Miklosovic et al., 2004). By contrast, previous studies of free-ranging bubble-net feeding animals have focused on their broader underwater behavior (Wiley et al., 2011; Szabo et al., 2024), coordinated group role specialization (Burrows, 2017), use of flippers (Kosma et al., 2019) and net structure (Szabo et al., 2024). Here, we focus on the fine-scale kinematics of solitary bubble-net feeding, empirically measuring the turning performance of free-swimming humpback whales. To contextualize our findings, we sourced recent data from a study that used biologging tags to document the positive allometry of maneuvering performance (i.e. accelerations, roll changes, turn types) across seven baleen whale species (Segre et al., 2022). From the Segre et al. (2022) study, we extracted data on the centripetal acceleration of all seven species. Because centripetal acceleration is directly correlated with the balance between speed and turn tightness, this metric effectively assesses the ability to generate radially directed force during turns, regardless of speed and trajectory variations (Segre et al., 2022). Centripetal acceleration therefore serves as a valuable metric for interspecific comparisons of turning performance, and to better understand why humpback whales are the only species documented to perform bubble-net feeding behaviors. We hypothesized that the large lift force generated by the humpback whale's uniquely large

pectoral flippers will result in them being the only species to perform the tight, high-speed, sustained turns required for solitary bubble-net feeding.

MATERIALS AND METHODS

Ethics

This study was conducted under NOAA permits issued to the Alaska Whale Foundation (no. 19703) and the Marine Mammal Research Program at the University of Hawai'i at Mānoa (no. 21476). All research was conducted under institution IACUC approvals.

Bubble-net feeding humpback whale tag and UAS data collection

Data were collected from small research vessels – a 10.3 m twin-engine aluminum vessel and a 5.9 m RHIB – at the confluence of Frederick Sound and lower Stephens Passage, northern Southeast Alaska (N57.4043, W133.5227), on 14–19 July 2019. Five randomly selected humpback whales engaging in solitary bubble-net feeding on krill were fitted with high-resolution suction-cup attached CATS (Customized Animal Tracking Solutions; www.cats.is) biologgers and an unoccupied aerial system (UAS; drone) was flown concurrently over three of the tagged animals (Table 1).

Tags were deployed following previously described methods (Cade et al., 2016; Segre et al., 2022). Whale responses to tagging were minimal, with foraging behavior resuming within seconds to minutes upon the tagging boat departing the animal's immediate vicinity. Sensors present in each tag included tri-axial accelerometers (400 Hz), gyroscopes (50 Hz), magnetometers (50 Hz), a high-resolution camera and a pressure sensor downsampled to 10 Hz, 16 bit. Using methods outlined by Cade et al. (2018), we quantified the swimming speed, roll (rotation about the longitudinal axis) and change in heading (yaw) during bubble-net production. Using the tag-derived videos, we measured the time at which bubble-net production was initiated and the duration of subsequent rings.

UAS video recordings (3840×2160 pixels, 29.97 frames s^{-1}) were obtained using a DJI Inspire 2 Pro multirotor UAS equipped with a 16 Megapixel Zenmuse X5 micro four-thirds camera with an Olympus M.Zuiko 25 mm *f*1.8 lens. We custom-fitted the UAS with a LightWare SF11/C laser range finder (Lightware Optoelectronics) with an accuracy of 10 cm (Christiansen et al., 2018) to measure its altitude above sea level. Whale length and structural elements of bubble-nets (i.e. radius and number of rings) were quantified via aerial photogrammetry methods outlined by Christiansen et al. (2018). From the UAS-derived diameter of each ring, the circumference was calculated by multiplying the diameter by π. Although calculations were performed for each ring in the bubble-net feeding sequence, analyses only included data from the first (outermost) and last (innermost) rings to maintain consistency across bubble-nets that may have varying numbers of rings (~2–6).

Body mass was estimated for tagged individuals with concurrent UAS data using the approach of Van Aswegen et al. (2025), which incorporates estimates of humpback whale body length, volume and condition to estimate body mass. The body volume estimate for each individual was partitioned into tissue-specific proportions, including bone, viscera (organs and connective tissue) and muscle, based on the structural length of each whale. The proportion of blubber was estimated using the whale's body condition, while body fluids (e.g. blood) were assumed to constitute 6% of the total body volume (Lockyer, 1976).

Kinematic calculations

Forward swimming speed of the animal (m s^{-1}) was estimated across the deployment using a regression between the magnitude of small-scale accelerometer 'jiggle' and orientation-corrected depth rate values. These methods are outlined in more detail by Cade et al. (2018). From our tag data, we also computed directional heading (i.e. yaw) using a tri-axial magnetometer, allowing us to verify the start, end, and duration of a given ring wherein the animal creates a single full circle. To compute the circumference of each innermost and outermost ring, we multiplied the forward swimming speed by the duration of ring creation. For a subset of bubble-nets (n=14; Table 1), UAS data was opportunistically collected for the entire duration of bubble-net production. For these nets, it was possible to verify the tag-derived swimming speed by dividing the circumference of each ring (m; measured by the UAS) by the duration of ring production (s), determined by positional changes in the tag data.

Centripetal acceleration ($\mathbf{a}_c$; m s^{-2}) was computed according to the equation:

$$\mathbf{a}_c = v^2/r, \quad (1)$$

where v and r represent the animal's velocity (m s^{-1}) and turning radius (m), respectively. Centripetal force could then be calculated for individuals with body mass estimates as:

$$\mathbf{F}_c = (m_b + 0.082\, m_b)\, \mathbf{a}_c, \quad (2)$$

where m_b represents the individual's body mass and 0.082 represents the added mass coefficient (Fish, 1999).

The maximum lift force ($\mathbf{F}_L$; N) generated by the pectoral flippers of the humpback whale was calculated (Eqn 3) assuming an ideal and commonly observed orientation (Fig. 1A), where the whale's roll angle (ϕ; deg) and the pectoral flipper rotational orientation (Ψ; deg) total 90 deg:

$$\mathbf{F}_L = 1/2\rho A\, C_L\, V^2. \quad (3)$$

In the above equation, ρ is the fluid density of seawater (1025 kg m^{-3}), A is the average planar area (m^2) of one side of both pectoral flippers (6.10 m^2; Woodward et al., 2006), C_L is the coefficient of lift (1.1) and V is the swimming speed (m s^{-1}) of the whale. In addition, a conservative estimate for lift force ($\mathbf{F}_{LS}$; N) was calculated (Eqn 4), assuming the flipper extended straight from the body without any additional rotation of the pectoral flipper to increase the angle of attack (Fig. 1B).

$$\mathbf{F}_{LS} = \mathbf{F}_L \cos(\phi) \quad (4)$$

Table 1. Summary of the tagging and UAS effort across the five solitary bubble-net feeding whales in the study

Deployment ID	Date	Duration (hh:mm)	Body length (m)	Body mass (kg)	Number of nets from tag	Number of nets from UAS
mn190714-42	14 Jul 2019	1:27	10.8	18,488	12	2
mn190714-54	14 Jul 2019	10:22	10.4	18,199	88	7
mn190718-42	18 Jul 2019	2:39	Unknown	Unknown	4	0
mn190718-54	18 Jul 2019	0:26	Unknown	Unknown	3	0
mn190719-54	19 Jul 2019	8:43	12.1	28,855	90	5
					Total=197	**Total=14**

Tagged whales that lacked subsequent UAS video were not measured nor was UAS data collected during their bubble-netting events.

Journal of Experimental Biology (2025) 228, jeb249607. doi:10.1242/jeb.249607

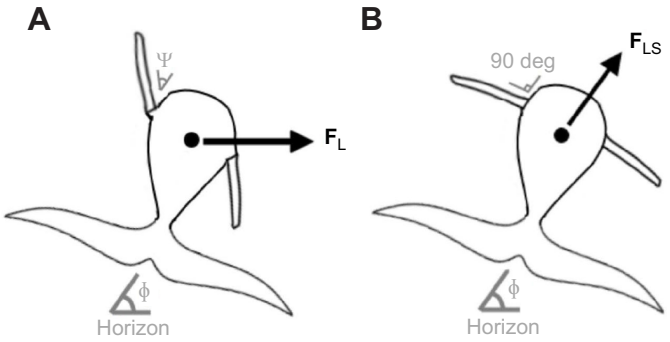

Fig. 1. Schematic of both flipper orientations during the turns of solitary bubble-net feeding humpback whales and the associated pectoral flipper lift force vectors. (A) Maximum lift force, F_L. (B) Conservative estimate for lift force, F_{LS}. ϕ represents the whale's roll angle relative to the horizon, and Ψ represents the pectoral flipper rotational orientation.

Although the total lift force remains the same in both orientations, when the flippers extend straight from the body (Fig. 1B), the lift vector is angled diagonally. In this case, only the horizontal component of the lift force contributes to centripetal force, while the vertical component does not aid in turning.

The coefficient of lift of a 14.6 m adult humpback whale was estimated via wind tunnel testing of an approximately 1:8 scale model of an excised pectoral flipper as described by Fassmann (2014). A series of images of the flipper, as it was partially suspended in air during necropsy, were used to create a 3D digital model that was then used to fabricate an oak model with a half-span of 0.5 m and a mean chord length of 0.15 m (Fig. 2). Owing to the absence of clear aerial images of the pectoral flippers of the solitary bubble-net feeding humpback whales in our study for direct morphological measurements, this individual's pectoral flipper model was used as their representative.

Lift data at angles of attack from −45 to +45 deg were acquired in a wind tunnel at a Reynolds number of Re≈430,000 based on mean chord length. The peak C_L=1.1 occurred at an angle of 16 deg. Since our modeling aims to demonstrate maximum lift forces across species, and minimal C_L values are largely unknown, we used the maximum C_L in our analysis to highlight peak performance and facilitate interspecific comparisons.

Sourced data

To contextualize the turning performance for these solitary bubble-net feeding humpback whales, we sourced data from seven large, free-ranging baleen whales (Segre et al., 2022) and seven smaller toothed whales under human care (Fish, 2002). The complete dataset from Segre et al. (2022) contained >100,000 turns (foraging and non-foraging); however, analyses in the present study include only longer duration turns (≥60 s) between 1 and 3 m s^{-1} (n=13,518 turns) that resemble those used during solitary bubble-net feeding behavior (Szabo et al., 2024). Data come from seven different mysticetes: the blue whale [*Balaenoptera musculus* (Linnaeus 1758); n=87 animals, n=7183 turns; California and Azores], inshore Bryde's whale (*Balaenoptera edeni* Anderson 1879; n=6 animals n=253 turns; South Africa), fin whale [*Balaenoptera physalus* (Linnaeus 1758); n=29 animals, n=1786 turns; Azores, California and Greenland], gray whale (*Eschrichtius robustus* Lilljeborg 1861; n=5 animals, n=198 turns; Washington), humpback whale [*Megaptera novaeangliae* (Borowski 1781); n=123 animals, n=3021 turns; various worldwide locations], Antarctic minke whale (*Balaenoptera bonaerensis* Burmeister 1867; n=20 animals, n=1000 turns; West Antarctic Peninsula) and sei whale (*Balaenoptera borealis* Lesson 1828; n=2 animals, n=77 turns; Falkland Islands). Given the large size and variability in the Segre et al. (2022) dataset, we did not investigate the circumstances of each outlier turn, instead choosing to report 5th and 95th percentile values sourced from this dataset (n=12,162 turns) as the 'minimum' and 'maximum', respectively, to avoid the effects of anomalous situations. Mean minimum turning radius values from seven odontocete species kept in human care facilities exhibiting powered turns were sourced from Fish (2002), including: the beluga whale [*Delphinapterus leucas*; n=2 animals, n=21 turns, Commerson's dolphin (*Cephalorhynchus commersonii*; n=3 animals, n=58 turns), Amazon river dolphin (*Inia geoffrensis*; n=1 animal, n=7 turns), white-beaked dolphin (*Lagenorhynchus albirostris*; n=4 animals, n=49 turns), killer whale (n=6 animals, n=31 turns), false killer whale (*Pseudorca crassidens*; n=3 animals, n=19 turns) and bottlenose dolphin (*Tursiops truncatus*; n=6 animals, n=41 turns). Ethical considerations and details on data collection methods for the sourced data may be found in their respective studies.

Statistical analyses

Paired t-tests were used to assess significant differences in mean radii, speeds and centripetal accelerations between the outer and innermost rings. A Shapiro–Wilk test was first run to check for a normal distribution of the data, then a square root transformation of the data was applied to meet this assumption. Given its robust nature to unequal sample sizes and non-homogenous variances, pairwise Welch's t-tests were used to compare the difference among the five tagged whales in mean radii, speeds and centripetal accelerations for both the outer and innermost rings. A Shapiro–Wilk test was first used to check for normal distribution, which was met in all of these cases. To test for significant differences in mean centripetal accelerations between the humpback whale and other mysticetes,

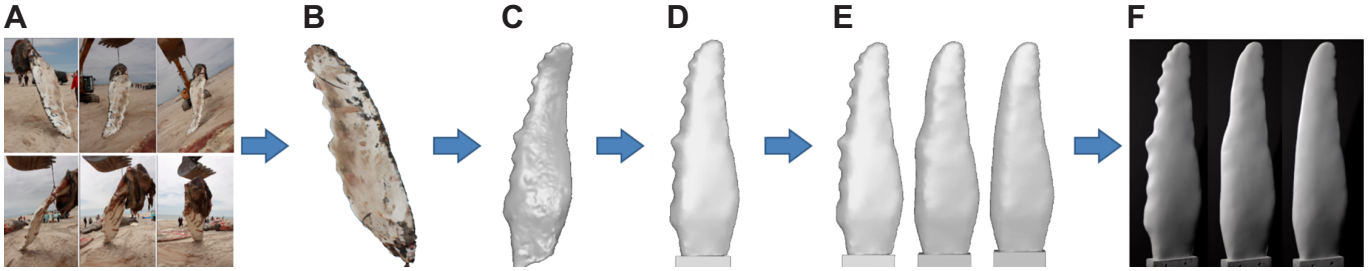

Fig. 2. Process overview for the 3D reconstruction of an adult humpback whale flipper. (A) Multi-view 2D images acquired of the humpback whale flipper; (B) 3D reconstructed flipper; (C–E) refined models and (F) fabricated 1:8 scale flipper model. Use of photos authorized under NMFS Permit No. 932-1905/MA-009526.

Journal of Experimental Biology (2025) 228, jeb249607. doi:10.1242/jeb.249607

Welch's *t*-tests were used because of unequal sample sizes. Data were square root transformed to meet the assumptions of a Welch's *t*-test. Significance levels were set to α=0.05 and average values are presented as means±s.e.m.

RESULTS

From our field efforts in Southeast Alaska, we documented 197 novel bubble-net feeding occurrences from five CATS tag deployments, including 14 nets from three whales with simultaneous UAS and tag data (Table 1). Dive durations of humpback whale bubble-net feeding events (n=197) ranged from 94 s to 258 s (mean=153±2 s), and bubble production durations ranged from 35 s to 193 s (mean±s.e.m.=96±2 s) (Fig. 3). Only 15 bubble-nets (7.6%) were produced in less than 60 s, the threshold used to subsample the Segre et al. (2022) dataset. Mean bubble production duration for the outer and innermost rings were 33±0.5 s and 21±0.2 s (means±s.e.m.), respectively. UAS photogrammetry-derived lengths of the three whales were 10.4 m, 10.8 m and 12.1 m (Table 1). The differences between the calculated mean swimming speeds from UAS imagery and the tag-derived data were negligible (<0.01 m s^{-1}) (Fig. S1); thus subsequent results and analyses incorporate only the tag data (n=5 whales; n=197 nets).

The average swimming speeds while producing the outer and innermost rings were 1.51±0.01 m s^{-1} and 1.50±0.01 m s^{-1}, respectively (means±s.e.m.). The speed ranged from 1.15 m s^{-1} to 1.82 m s^{-1} in the outermost ring and from 1.02 m s^{-1} to 1.69 m s^{-1} in the innermost ring. A paired *t*-test (t_{196}=1.0117; P=0.31) showed no significant difference in speed between the outer and innermost rings. Speed differed significantly among three whales for the outermost ring (Welch's *t*-test; P<0.02), and four whales for the innermost ring (Welch's *t*-test; P<0.01).

Average radii of the outermost and innermost rings of bubble-net feeding events were 7.85±0.12 m and 4.96±0.05 m, respectively (means±s.e.m.). Radii ranged from 4.27 m to 13.85 m for the outermost ring, and 3.25 m to 7.81 m for the innermost ring. The radii between the outermost and innermost rings were significantly different (paired *t*-test, t_{196}=25.747; P<0.001). There was no significant difference in the radius of the outermost ring among any of the whales (Welch's *t*-test; P>0.48), but there were significant differences between the radii of the innermost rings among four whales (Welch's *t*-test; P<0.04). Given the average length of the three solitary bubble-net feeding whales with UAS data (11.1 m), the mean turning radius of the innermost ring (4.96 m) can be converted to a length-specific turning radius (0.45 lengths) (Fig. 4). The only delphinid with a smaller length-specific turning radius was the Amazon river dolphin (0.33 lengths; 0.84 m) (Fig. 4). The smallest length-specific turning radius came from the humpback whale data in Segre et al. (2022), which exhibited a minimum length-specific turning radius of 0.14 lengths (1.96 m) (Fig. 4).

Centripetal acceleration was calculated for both the outer (0.30±0.00 m s^{-2}) and innermost (0.46±0.01 m s^{-2}) rings (means±s.e.m.; Fig. 5), ranging from 0.17 m s^{-2} to 0.55 m s^{-2} for the outermost ring and 0.25 m s^{-2} to 0.73 m s^{-2} for the innermost ring. Centripetal acceleration differed significantly between the outer and innermost rings (paired *t*-test, t_{196}=−23.734; P<0.001). Three whales had significantly different centripetal accelerations for the outermost (Welch's *t*-test; P<0.01) and innermost (Welch's *t*-test; P<0.01) rings.

Fig. 6 outlines the range of each species (5–95%) for centripetal accelerations from the Segre et al. (2022) dataset during turns that resemble solitary bubble-net feeding (duration ≥60 s; speed between 1 and 3 m s^{-1}). Within this dataset, we found significant differences in mean centripetal accelerations between humpback whales and all other species examined (Table S1). Comparing our dataset of solitary bubble-net feeding humpback whales against these broader data, we found the mean centripetal acceleration of the innermost ring to be above the upper limit for all species except the humpback whale, which displayed a maximum centripetal acceleration (95th percentile; 1.40 m s^{-2}) over three times greater than the average value for the innermost ring (0.46 m s^{-2}) (Fig. 6).

Centripetal force was calculated for the three individuals with body mass estimates (n=190 bubble-netting events) as 7730±196 N for the outermost ring and 11,585±190 N (means±s.e.m.) for the innermost ring. Centripetal force ranged from 3429 N to 14,700 N

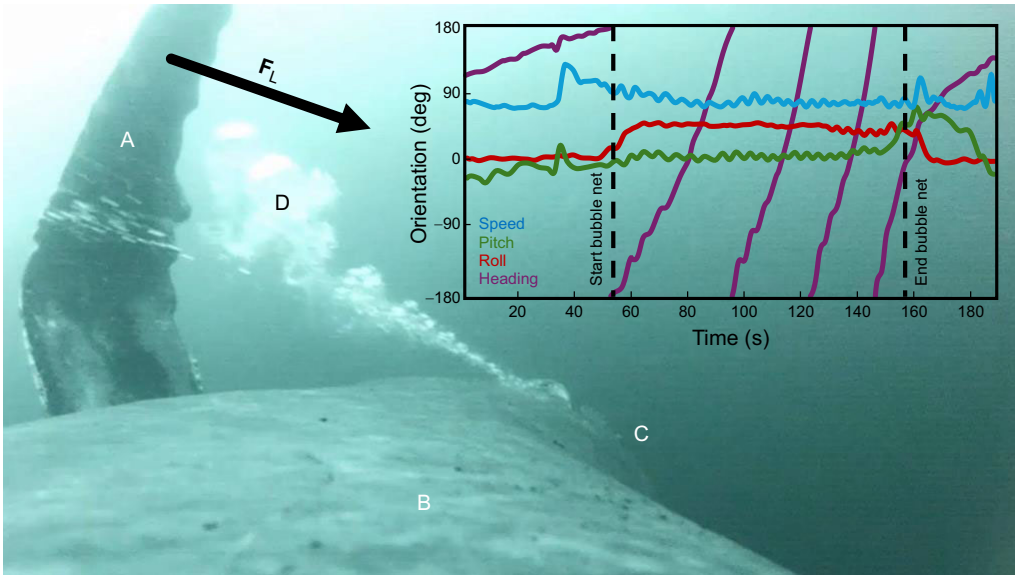

Fig. 3. Screenshot of a solitary bubble-net feeding humpback whale from a CATS tag deployment. At the moment captured in the screenshot, the whale's roll is 46 deg, pitch is 0 deg and heading is 88 deg. The labeled features include: (A) pectoral flipper, (B) dorsal side of the body, (C) head and (D) bubbles. The arrow denotes the direction of the lift force ($\mathbf{F}_L$). The corresponding tag data (smoothed for clarity) from the depicted bubble-netting event is shown at top right.

Journal of Experimental Biology (2025) 228, jeb249607. doi:10.1242/jeb.249607

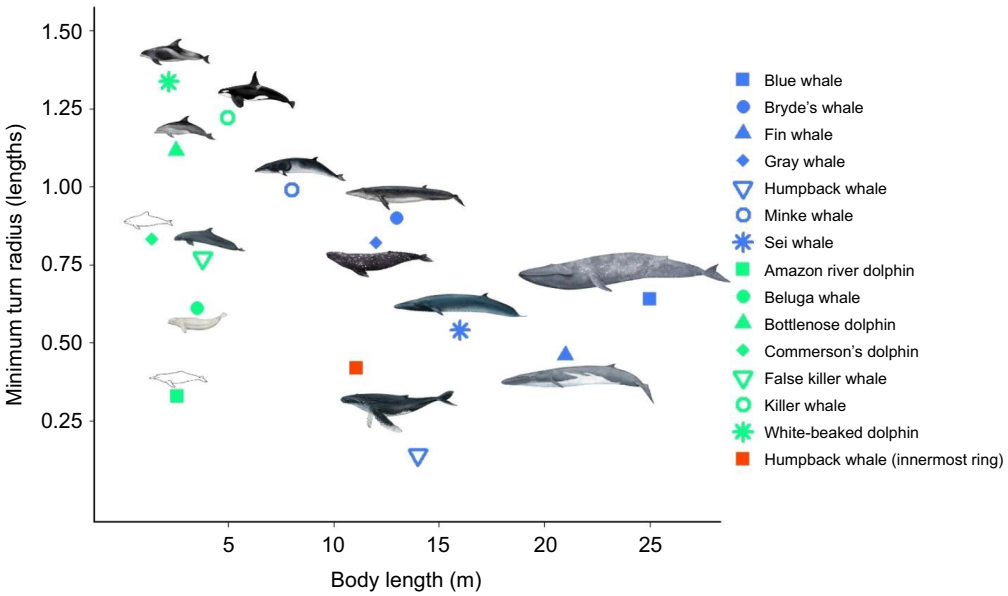

Fig. 4. Minimum length-specific turning radii. Seven mysticetes (blue; 5th percentile; Segre et al., 2022) and seven odontocetes (green; Fish, 2002) along with the mean turning radius of the innermost ring during solitary bubble net feeding (red; present study). Average length of the mysticetes and odontocetes come from their respective studies. The length of the solitary bubble-net feeding humpback whale is represented by the average of the three whales with concurrent UAS and tag data.

for the outermost ring and from 5632 N to 18,710 N for the innermost ring. Centripetal force differed significantly between the outer and innermost rings (paired *t*-test, t_{189}=−24.767; P<0.001). All three whales differed significantly in the centripetal forces generated during the formation of both the outermost (Welch's *t*-test; P<0.01) and innermost (Welch's *t*-test; P<0.01) rings.

Mean (±s.e.m.) roll during bubble-netting events was 40.30±0.46 deg (95% range: 23.99–50.58 deg). Maximum roll was 59.75±0.58 deg on average (95% range: 48.54–79.05 deg). Average roll was significantly different for two whales (Welch's *t*-test; P<0.001), and maximum roll differed significantly between two whales (Welch's *t*-test; P<0.001).

Assuming an ideal orientation ($\phi+\Psi$=90 deg), the pectoral flippers generated a mean (±s.e.m.) calculated lift force of 7857±81 N for the outermost ring and 7800±85 N for the innermost ring. With its pectoral flippers extended straight out from the body at an average roll angle of 40 deg, the lift force exerted by the humpback whale's pectoral flippers was calculated as 6018 ±62 N and 5975±65 N for the outer and innermost rings, respectively. The calculated lift forces that humpback whale pectoral flippers are capable of generating are considerably larger than those of other cetaceans with known lift coefficients and pectoral flipper planar areas (Table 2).

DISCUSSION

This study demonstrates that solitary bubble-net krill-feeding humpback whales exhibit a turning performance that exceeds the observed capabilities of all other mysticetes that have been measured. Even at higher speeds or shorter durations, the other baleen whales examined in this study lacked the turning performance needed to create the innermost ring during solitary bubble-net feeding, with only the minke and fin whales approaching this requirement. This likely occurs as a result of the smaller size of the minke whale lending itself to enhanced maneuverability (Segre et al., 2022) and the capability of fin whales to achieve comparatively high speeds (and thus high centripetal accelerations) (Bose and Lien, 1989; Ford and Reeves, 2008). However, fin and minke whale performance differs from the humpback whale in that the centripetal accelerations for these species are at the upper extremity of their capabilities. Species that approach the turning requirements of solitary bubble-net feeding,

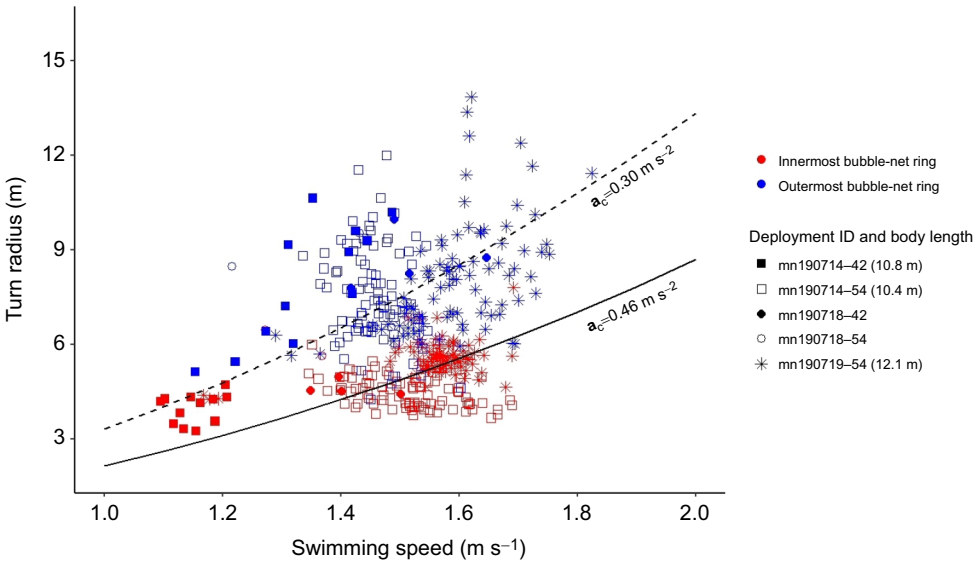

Fig. 5. Scatterplot of humpback whale solitary bubble-net feeding events. Data are from 197 feeding events depicting the swimming speed and turn radius for both the outermost (blue) and innermost (red) rings. Two constant centripetal acceleration lines are plotted, using mean values from the outermost (dashed) and innermost (solid) rings. Points located below or to the right of these constant centripetal acceleration lines indicate above average centripetal accelerations, resulting from a tighter turning radius or a higher swimming speed, respectively. Points above or to the left of the constant centripetal acceleration lines indicate below average centripetal accelerations, resulting from a wider turning radius or a lower swimming speed, respectively.

Journal of Experimental Biology (2025) 228, jeb249607. doi:10.1242/jeb.249607

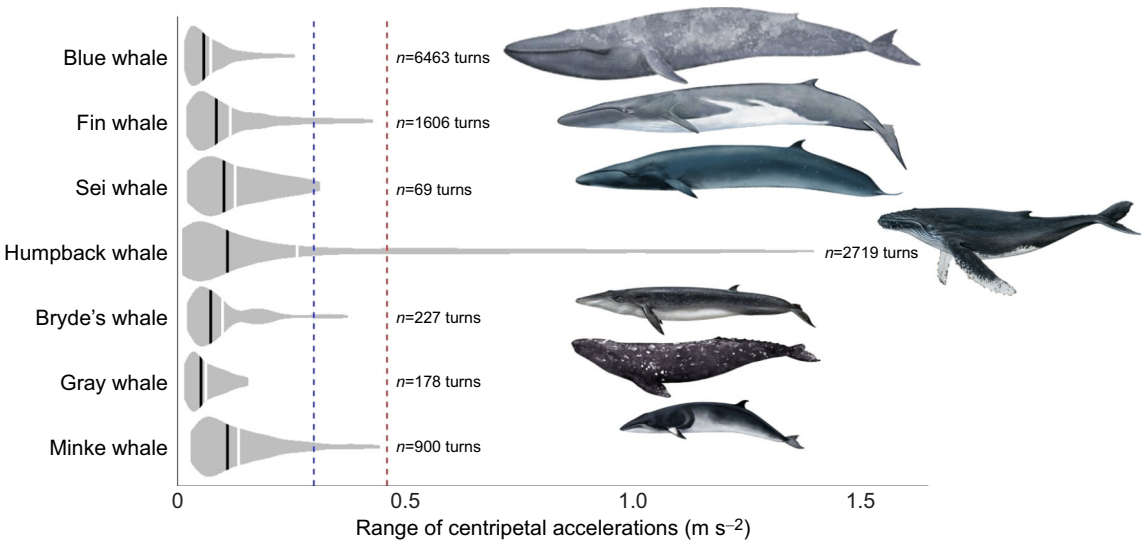

Fig. 6. Violin plot depicting the range (5–95%) of centripetal accelerations. Data are recorded from tags of the seven mysticetes reported in Segre et al. (2022) for turns with a duration of at least 60 s, between an average speed of 1 and 3 m s^{-1} (n=12,162 turns). Species are listed in order of increasing body length (starting from the bottom). The dashed blue and red lines represent the mean centripetal acceleration utilized during solitary bubble-net feeding (present study) for the outer and innermost rings, respectively. The species-specific mean (white) and median (black) centripetal accelerations are represented by the solid bars in each range.

along with those that have a rare anomaly beyond the 5–95% range (Segre et al., 2022), may represent a scenario where creating a bubble-net structure is physically possible, but the energetic cost associated with doing so would outweigh the energetic benefit of corralling higher prey densities in bubble-nets (Allen et al., 2024; Szabo et al., 2024; Wiley et al., 2011).

From the complete Segre et al. (2022) dataset, all species achieved much greater centripetal accelerations (>200%) than required for solitary bubble-net feeding, but these most often occurred during powered turns performed at high speeds for long durations (resulting in large-radius turns) or unpowered turns performed over very short durations. The fact that over 92% of bubble-nets took more than 60 s to produce suggests an energetic advantage of sustained turning that supersedes the additional locomotor costs. Other species may be unable to achieve a favorable mix of high centripetal acceleration and low turning radius to efficiently use solitary bubble-net feeding as a foraging tactic. However, other baleen whales targeting krill have been shown to employ alternative strategies to optimize foraging efficiency, such as targeting deeper, denser prey patches (D'Agostino et al., 2024; Friedlaender et al., 2020) or adjusting the number of lunges per dive based on prey density (Hazen et al., 2015).

The mean centripetal acceleration employed during the innermost ring is below the midpoint of the observed range for humpback whales (Fig. 6), indicating that these whales can achieve even greater turning performance. This is observed in Fig. 4, where the minimum (5th percentile) turning radius reported for humpback whales from the subset of data in Segre et al. (2022) (1.96 m) was less than half of the mean radius of the innermost ring during solitary bubble-net feeding (4.96 m). While the Segre et al. (2022) dataset encompasses a wide variety of behaviors (foraging and non-foraging), investigating the specific behaviors driving extreme centripetal accelerations in humpback whales was beyond the scope of this study. As the fine-scale behaviors of bubble-net feeding varies across populations (Allen et al., 2024; Burrows, 2017; Mastick et al., 2022; Szabo et al., 2024), a plausible explanation is that these higher centripetal accelerations come from bubble-net feeding humpback whales targeting more mobile prey types (e.g. Pacific herring) (Jurasz and Jurasz, 1979).

The tight turning radius generated during solitary bubble-net feeding is remarkable, especially in the context of the humpback whale's massive size (Fig. 4). The length-specific radius generated during bubble-net feeding of the humpback whale is within the range for maximum turning performance (Fish, 2002) of smaller, toothed whales (Fig. 4). The humpback whale's length-specific turning radius (0.45 body lengths) during the innermost ring was smaller than the minimum length-specific turning radius of all

Table 2. Calculated lift forces at solitary humpback whale bubble-net feeding speed (innermost ring) for species with known pectoral flipper planar areas and lift coefficients

Species	Length (m)	Pectoral flipper planar area (m^2)	Speed (m s^{-1})	Lift coefficient	F_L (N)	F_{LS} (N)
Humpback whale (*Megaptera novaeangliae*)	13.5	6.10	1.50	1.100	**7800**	5975
Fin whale* (*Balaenoptera physalus*)	14.4	0.24	1.50	1.452	**402**	308
Minke whale (*Balaenoptera bonaerensis*)	8.0	0.18	1.50	1.500	**311**	238
Killer whale (*Orcinus orca*)	6.5	0.41	1.50	1.040	**492**	377
Sperm whale (*Physeter macrocephalus*)	12.0	0.55	1.50	0.897	**569**	436

All whales were adults and information on the animal's sex was only available for the killer whale (female; Weber et al., 2014). Length, pectoral flipper planar area and lift coefficient data for the fin whale, killer whale and sperm whale are sourced from Weber et al. (2014). Pectoral flipper planar area and lift coefficient data for the minke whale are from Cooper et al. (2008). Length data for the minke and humpback whales are from Segre et al. (2022) and Woodward et al. (2006), respectively. *Data provided for the fin whale are from an animal smaller than the average adult body length (~21 m) for the species. F_L, maximum lift force; F_{LS}, conservative estimate for lift force.

odontocetes (Fish, 2002) except the Amazon river dolphin (0.33 body lengths), which benefits from a flexible body and low-speed maneuvering suited to its complex habitat (Fish, 2002). Solitary bubble-net feeding does not represent the extreme of a humpback whales' turning capability (Fig. 6) and is clearly seen in Fig. 4, where the smallest length-specific turning radius overall comes from the humpback whales from the subset of turns in Segre et al. (2022). This exemplifies how humpback whales can compensate for their greater length and mass through their elongate pectoral flippers.

The high centripetal accelerations utilized in solitary bubble-net feeding, especially as the radius decreases, results from the humpback whale's ability to maintain its speed throughout the duration of the bubble-net feeding event. We found no significant difference in swimming speed between the outer and innermost rings, suggesting that these bubble-net feeding events represent powered turns where the thrust derived from propulsive fluking propels the whale through consecutive rings. The presence of fluke strokes during bubble production was visually confirmed using accelerometer data from the tags. With maintenance of a constant velocity, the decreasing radius of the turn is therefore a function of increasing lift, which increases with the square of velocity. By increasing the bank angle, turning further increases centripetal force from the pectoral flippers. The increased lift can also come from an increase in the angle of attack of the flippers. This maintained velocity differs from that of delphinid species, as they commonly limit or disengage propulsion entirely to flex the body and achieve tighter radius turns, thus limiting speed and acceleration upon completion of a turn (Fish, 2002). Blue whales, however, show no significant difference in turning velocity between powered and unpowered turns, and tighten their turns by banking inwards and using their spinal flexibility to reduce the turn radius (Segre et al., 2019). Therefore, the ability to roll their bodies and arch into a turn is important for large whales, such as blue whales and humpback whales, when needing to quickly reduce their turning radius.

A large planar surface area of the pectoral flippers aids in generating a large lift force, as evidenced by humpback whales generating more lift than both the larger fin and sperm whales, and smaller minke and killer whales (Table 2). A humpback whale measuring 13.5 m in length and in average body condition would have an estimated mass of 33,286 kg (Van Aswegen et al., 2025) and would therefore generate 16,567 N of centripetal force during creation of the innermost ring, assuming the average centripetal acceleration of 0.46 m s^{-2} and an added mass coefficient of 0.082. Given that the lift produced by the pectoral flippers is estimated at between 5975 N and 7800 N for a humpback whale of this size (depending on flipper orientation), flipper-generated lift would account for approximately 36–47% of the total force required to form the innermost ring. Using published length to weight relationships (Lockyer, 1976), we can model the centripetal force generated by minke and fin whales during the formation of the innermost ring at the average centripetal acceleration of 0.46 m s^{-2} as 3009 N and 9102 N, respectively. The maximum lift forces produced by their flippers were estimated at 311 N for minke whales and 402 N for fin whales, accounting for approximately 10% and 4% of the total force required, respectively. The reduced lift forces generated by the pectoral flippers of other whales require them to generate significant lift through other active mechanisms such as the use of their flukes as a control surface, and increased bank angles, angle of attack of the flippers and spinal flexion. These mechanisms would likely increase energetic expenditure. However, spinal flexibility is limited, the angle of attack of the flippers is limited by stall, and the bank angle is limited at 90 deg.

We based the pectoral flipper planar area (6.10 m^2) on a sample with a mean body length of 13.5 m (Woodward et al., 2006), which likely overestimates the area for the 11.1 m average body length in our study. While this suggests the lift forces might be somewhat overestimated, the high lift generated by humpback whale pectoral flippers still far exceeds that of other cetaceans, minimizing the impact of this difference. Throughout the production of a bubble-net, the whale must maneuver its body into a sufficient angle to bank inwards and decrease its turning radius, while propelling itself quickly enough to avoid prey escape. When rolled, the extension of their pectoral flippers contributes to centripetal acceleration by providing a lift force oriented towards the center of the turning radius (Fig. 3). The lift force is minimized when the pectoral flipper extends straight out from the body with no additional rotation ($\mathbf{F}_{LS}$) and is maximized when the roll angle of the whale's body and the pectoral flipper rotational orientation total 90 deg ($\mathbf{F}_{L}$) (Table 2). By calculating both extremes, we show the range of possible lift force generation during solitary bubble-net feeding. However, the most common orientation during bubble-net production resembles the whale's roll angle and the pectoral flipper rotation totaling 90 deg (Fig. 1A). It is difficult to accurately measure the flipper's angle of attack without placing a tag directly on the flipper, although visual analysis of the tag video suggests this estimate is reasonable. Logically, this ideal orientation makes sense given the massive size of a humpback whale and the small radius they must achieve for solitary bubble-net feeding. The large lift force generated by their pectoral flippers can be leveraged by humpback whales in tandem with their spinal flexibility to decrease turning radius, whereas other baleen whales lacking substantial lift force from the flippers may rely primarily on their spinal flexibility (Segre et al., 2019). After creating the bubble-net, the whale then slows down and maneuvers itself into a vertical orientation to lunge up through the net and engulf prey (Szabo et al., 2024). Being able to efficiently maneuver at low speeds is difficult owing to a reduction in velocity-dependent lift generation relative to the centripetal force needed to turn (Fish, 2002). The large planar area of the humpback whale's pectoral flippers allows for more effective maneuvering at low speeds, which is important to quickly transition to the lunging phase of this feeding strategy.

Our lift coefficient (1.1) was obtained from a 14.6 m humpback whale, which is larger than the 11.1 m average body length of the solitary bubble-net feeding humpback whales in the present study. However, this lift coefficient is comparable to that used by Fish and Battle (1995) for a 9 m humpback whale (1.3), suggesting that variations in lift force due to differences in lift coefficients across different whale sizes are minimal. Assuming a maximum lift coefficient enhances the accuracy of modeling peak lift forces. This assumption may overestimate lift when the animal's angle of attack is suboptimal for generating maximum lift. As we aimed to estimate the maximum lift forces generated by humpback whale pectoral flippers, we used these maximum lift coefficients, while recognizing that the flippers' angle of attack and force estimate may vary within a single net or between different nets depending on turning requirements.

One of the defining characteristics of humpback whale pectoral flippers is the presence of large tubercles or bumps along the leading edge, giving the flipper a scalloped appearance. These tubercles delay stall by providing greater lift at higher angles of attack (Fish and Battle, 1995; Miklosovic et al., 2004). The high lift-generating performance of the tubercled flippers can produce a large lift disparity between counter-rotated pectoral flippers (i.e. high positive lift on one and high negative lift on the other), enhancing

rolling ability and resulting in higher rolling speeds (Goldbogen et al., 2013; Segre et al., 2016; Weihs, 1993). This utilization of roll is clearly observed in solitary bubble-net feeding, with the animal banking to ∼40 deg and maintaining a consistent level of roll throughout bubble production (Fig. 3). This relatively consistent roll differs from the findings in Wiley et al. (2011), where bubble-net feeding groups of humpback whales in the Gulf of Maine had greater fluctuations in roll through the production of a bubble-net. The need for more frequent adjustments in roll angle may be driven by the necessity to better target and prevent the escape of the more mobile prey (e.g. small fish) that humpback whales typically feed upon in the Gulf of Maine (Hain et al., 1982; Hazen et al., 2009; Payne et al., 1990). Furthermore, the whales in Wiley et al. (2011) were feeding in groups, so it is possible that some maneuvering was associated with proximity to other whales. Quickly adjusting their roll may be particularly challenging for other mysticetes, which lack the large pectoral flippers and leading-edge tubercles that enhance the maneuverability of humpback whales (Fish and Battle, 1995). Given the average roll of 40 deg, the mean turning radius of the innermost ring (4.96 m) is even tighter than predictions by prior models that assessed the turning radius achieved by the humpback whale's pectoral flippers alone as a function of roll angle (Fish, 2004; Fish and Battle, 1995). At a maximum roll angle of 90 deg, based only on the use of the flippers, Fish and Battle (1995) predicted that a 9 m humpback whale would have a minimum turning radius of 7.4 m. According to this model, the same 9 m whale at a bank angle of 40 deg would generate a turning radius of 11.5 m. The larger whales in the present study were thus able to achieve a tighter turning radius by using their dorso-ventral flexibility (Segre et al., 2019) to arch their bodies into the center of the turn. Additionally, the flexibility of their pectoral flippers (Edel and Winn, 1978) likely contributes to this maneuverability. Even when the whale is oriented at a particular angle, the pectoral flippers may flex and achieve an even greater angle of attack, thereby directing the lift force further inward (Fig. 3).

As our study had a small sample size of three whales measured via UAS, we lacked the power to assess the impact of body size on the kinematics of solitary bubble-net feeding. However, it is notable that these humpback whales are below the average adult size (∼13 m; Clapham, 1996) and well below the maximum recorded length (17.4 m; Chittleborough, 1965). Future research should explore whether body size has a significant effect on these kinematic parameters associated with bubble-net feeding and how the fine-scale kinematics of bubble-net feeding may differ in coordinated groups (but see Burrows, 2017). The kinematic demands of cooperative bubble-net feeding may be more aligned with the turning capacity of other baleen whales and could potentially develop as a foraging strategy in other species, particularly as they adapt to targeting fewer or less dense prey patches due to climate change (Flores et al., 2012; McBride et al., 2021) and increases in commercial fishing (Nicol et al., 2012). Furthermore, considering that foraging requirements vary across populations, prey types and prey density (Cade et al., 2016; Goldbogen et al., 2015), future research should explore the kinematic demands – both solitary and cooperatively – of other bubble-net feeding populations and how these demands change with respect to prey type and density. Given that this foraging tactic has been documented amongst humpback whales attempting to maximize energetic gain across a feeding season (Szabo et al., 2024), a deeper understanding of the kinematic requirements and energetic cost of this foraging strategy is necessary to refine our understanding of energy budgets in these animals.

Our study examined the fine-scale kinematics of one of the most complex foraging behaviors in the animal kingdom (Szabo et al., 2024). Our results show that humpback whales exhibit greater centripetal accelerations during solitary bubble-net feeding than the observed centripetal accelerations in the other baleen whales examined, suggesting that they may be uniquely capable of performing the complex maneuvers required for this behavior. While we cannot definitively assess the maximum physical capabilities of the species examined because of the observational nature of the data, baleen whales demonstrate remarkable maneuverability for their size (Segre et al., 2022). It is possible that some mysticetes may be able to achieve the necessary turning performance for solitary bubble-net feeding, although the energetic costs may exceed the benefits of the higher prey densities associated with bubble-net feeding. Owing to their unique morphology (e.g. large pectoral flippers, flukes and presence of tubercles), humpback whales generate the substantial lift force and centripetal acceleration necessary for this distinctive foraging tactic. Because humpback whales have evolved a unique morphology that allows them to perform tight, high-speed, sustained turns, they are exceptionally well suited to exploit less dense aggregations of prey through specialized foraging strategies such as solitary bubble-net feeding.

Acknowledgements
We thank our funders, including: the Undergraduate Research Opportunities Program at the University of Hawai'i at Mānoa, the University of Hawai'i at Mānoa, DoD's Defense University Research Instrumentation Program, the Omidyar Ohana Foundation, and the Lindblad Expedition-National Geographic Fund. We also thank the members of the Marine Mammal Research Program and the Hawai'i Institute of Marine Biology for their logistical support. We are grateful for the numerous people who contributed data to our study, including: Edward A. Roualdes, David E. Cade, Max F. Czapanskiy, James Fahlbusch, Shirel R. Kahane-Rapport, William K. Oestreich, K. C. Bierlich, John Calambokidis, John W. Durban, Holly Fearnbach, Peter Hegelund, David W. Johnston, Douglas P. Nowacek, Machiel G. Oudejans, Gwenith S. Penry, Jean Potvin, Andrew Stanworth, and David N. Wiley; Mahalo Kaipo L. for editing the Hawaiian translation of the abstract. This paper represents HIMB and SOEST contribution numbers 1999 and 11964, respectively.

Competing interests
The authors declare no competing or financial interests.

Author contributions
Conceptualization: C.N., W.T.G.; Data curation: W.T.G., P.S.S., F.E.F., A.S.; Formal analysis: C.N., W.T.G., M.v.A.; Funding acquisition: A.S., L.B., J.A.G.; Investigation: C.N., P.S.S., F.E.F., A.S., W.N.F., S.L.T., M.v.A., L.B.; Methodology: C.N., W.T.G., F.E.F., A.S., W.N.F., S.L.T., M.v.A., J.A.G.; Project administration: L.B.; Resources: P.S.S., F.E.F., A.S., L.B., J.A.G.; Supervision: L.B., J.A.G.; Validation: C.N., P.S.S., F.E.F., A.S., L.B.; Visualization: C.N., W.T.G., F.E.F.; Writing – original draft: C.N., W.T.G.; Writing – review & editing: C.N., W.T.G., P.S.S., F.E.F., A.S., W.N.F., S.L.T., M.v.A., J.A.B., E.M.C., J.d.C., A.S.F., J.A.G., M.S., J.M.S., S.K.A.V., F.V., C.R.W., L.B.

Funding
Funding for this study was provided by the University of Hawai'i at Mānoa, the U.S. Department of Defense [Defense University Research Equipment Program (DURIP) #N00014-19-2-2612], the Omidyar Ohana Foundation, the Lindblad Expedition-National Geographic Fund and the National Science Foundation (NSF IOS-1656691).

Data and resource availability
All relevant data can be found within the article and its supplementary information.

ECR Spotlight
This article has an associated ECR Spotlight interview with Cameron Nemeth.

References
Acevedo, J., Plana, J., Aguayo-Lobo, A. and Pastene, L. (2011). Surface feeding behavior of humpback whales in the Magellan Strait. *Rev. Biol. Mar. Oceanogr.* **46**, 483-490. doi:10.4067/S0718-19572011000300001

Allen, J., Nichols, R., Pallin, L., Johnston, D. and Friedlaender, A. (2024). Use and prevalence of novel bubble-net foraging strategy in Western Antarctic humpback whales. *Mar. Ecol. Prog. Ser.* **743**, 97-111. doi:10.3354/meps14654

Bird, C. N., Pirotta, E., New, L., Bierlich, K. C., Hildebrand, L., Fernandez Ajó, A. and Torres, L. G. (2024). Bubble blasts! An adaptation for buoyancy regulation in shallow foraging gray whales. *Ecol. Evol.* **14**, e70093. doi:10.1002/ece3.70093
Bose, N. and Lien, J. (1989). Propulsion of a fin whale (*Balenoptera physalus*): why the fin whale is a fast swimmer. *Proc. R. Soc. Lond. B. Biol. Sci.* **237**, 175-200. doi:10.1098/rspb.1989.0043
Burrows, J. A. (2017). Fine-scale foraging behavior of humpback whales (*Megaptera novaeangliae*) in Southeast Alaska. *PhD Thesis*, Duke University, Durham, NC.
Burrows, J. A., Johnston, D. W., Straley, J. M., Chenoweth, E. M., Ware, C., Curtice, C., Deruiter, S. L. and Friedlaender, A. S. (2016). Prey density and depth affect the fine-scale foraging behavior of humpback whales *Megaptera novaeangliae* in Sitka Sound, Alaska, USA. *Mar. Ecol. Prog. Ser.* **561**, 245-260. doi:10.3354/meps11906
Cade, D. E., Friedlaender, A. S., Calambokidis, J. and Goldbogen, J. A. (2016). Kinematic diversity in rorqual whale feeding mechanisms. *Curr. Biol.* **26**, 2617-2624. doi:10.1016/j.cub.2016.07.037
Cade, D. E., Barr, K. R., Calambokidis, J., Friedlaender, A. S. and Goldbogen, J. A. (2018). Determining forward speed from accelerometer jiggle in aquatic environments. *J. Exp. Biol.* **221**, jeb170449. doi:10.1242/jeb.170449
Cade, D. E., Carey, N., Domenici, P., Potvin, J. and Goldbogen, J. A. (2020). Predator-informed looming stimulus experiments reveal how large filter feeding whales capture highly maneuverable forage fish. *Proc. Natl. Acad. Sci. USA* **117**, 472-478. doi:10.1073/pnas.1911099116
Cade, D. E., Kahane-Rapport, S. R., Wallis, B., Goldbogen, J. A. and Friedlaender, A. S. (2022). Evidence for size-selective predation by Antarctic humpback whales. *Front. Mar. Sci.* **9**, 747788. doi:10.3389/fmars.2022.747788
Chenoweth, E. M., Boswell, K. M., Friedlaender, A. S., McPhee, M. V., Burrows, J. A., Heintz, R. A. and Straley, J. M. (2021). Confronting assumptions about prey selection by lunge–feeding whales using a process–based model. *Funct. Ecol.* **35**, 1722-1734. doi:10.1111/1365-2435.13852
Chittleborough, R. G. (1965). Dynamics of two populations of the humpback whale, *Megaptera novaeangliae* (Borowski). *Aust. J. Mar. Freshw. Res.* **16**, 33-128. doi:10.1071/MF9650033
Christiansen, F., Vivier, F., Charlton, C., Ward, R., Amerson, A., Burnell, S. and Bejder, L. (2018). Maternal body size and condition determine calf growth rates in southern right whales. *Mar. Ecol. Prog. Ser.* **592**, 267-281. doi:10.3354/meps12522
Clapham, P. J. (1996). The social and reproductive biology of Humpback Whales: an ecological perspective. *Mamm. Rev.* **26**, 27-49. doi:10.1111/j.1365-2907.1996.tb00145.x
Clapham, P. J. and Mead, J. G. (1999). *Megaptera novaeangliae*. *Mamm. Species* **604**, 1-9. doi:10.2307/3504352
Cooper, L. N., Sedano, N., Johansson, S., May, B., Brown, J. D., Holliday, C. M., Kot, B. W. and Fish, F. E. (2008). Hydrodynamic performance of the minke whale (*Balaenoptera acutorostrata*) flipper. *J. Exp. Biol.* **211**, 1859-1867. doi:10.1242/jeb.014134
D'Agostino, V. C., Nocera, A. C., Abernathy, K., Wilson, A. M., Coscarella, M. A. and Degrati, M. (2024). Foraging dives of southern right whales (*Eubalaena australis*) in relation to larger zooplankton size prey availability in Golfo Nuevo, Península Valdés, Argentina. *Sci. Rep.* **14**, 14211. doi:10.1038/s41598-024-63879-y
Edel, R. K. and Winn, H. E. (1978). Observations on underwater locomotion and flipper movement of the humpback whale *Megaptera novaeangliae*. *Mar. Biol.* **48**, 279-287. doi:10.1007/BF00397155
Fassmann, W. N. (2014). An experimental study of bio-inspired force generation by unsteady flow features. *M.S. Thesis*, Brigham Young University, Provo, UT.
Fish, F. E. (1993). Influence of hydrodynamic design and propulsive mode on mammalian swimming energetics. *Austral. J. Zool.* **42**, 79-101. doi:10.1071/ZO9940079
Fish, F. E. (1999). Performance constraints on the maneuverability of flexible and rigid biological systems. In: Proceedings of the Eleventh International Symposium on Unmanned Untethered Submersible Technology. Autonomous Undersea Systems Institute, Durham, New Hampshire.
Fish, F. E. (2002). Balancing requirements for stability and maneuverability in cetaceans. *Integr. Comp. Biol.* **42**, 85-93. doi:10.1093/icb/42.1.85
Fish, F. E. (2004). Structure and mechanics of nonpiscine control surfaces. *IEEE J. Oceanic Eng.* **29**, 605-621. doi:10.1109/JOE.2004.833213
Fish, F. E. and Battle, J. M. (1995). Hydrodynamic design of the humpback whale flipper. *J. Morphol.* **225**, 51-60. doi:10.1002/jmor.1052250105
Fish, F. E. and Hui, C. A. (1991). Dolphin swimming–a review. *Mamm. Rev.* **21**, 181-195. doi:10.1111/j.1365-2907.1991.tb00292.x
Fish, F. E. and Lauder, G. V. (2017). Control surfaces of aquatic vertebrates in relation to swimming modes. *J. Exp. Biol.* **220**, 4351-4363. doi:10.1242/jeb.243224
Fish, F. E. and Rohr, J. J. (1999). Review of dolphin hydrodynamics and swimming performance. In: SPAWARS System Center Technical Report. San Diego, CA: SSC.
Fish, F. E., Smelstoys, J. and Baudinette, R. V. (2002). Fur does not fly, it floats: buoyancy of pelage in semi-aquatic mammals. *Aquat. Mamm.* **28.2**, 103-112.
Fish, F. E., Legac, P., Williams, T. M. and Wei, T. (2014). Measurement of hydrodynamic force generation by swimming dolphins using bubble DPIV. *J. Exp. Biol.* **217**, 252-260. doi:10.1242/jeb.087924
Flores, H., Atkinson, A., Kawaguchi, S., Krafft, B., Milinevsky, G., Nicol, S., Reiss, C., Tarling, G., Werner, R., Bravo Rebolledo, E. et al. (2012). Impact of climate change on Antarctic krill. *Mar. Ecol. Prog. Ser.* **458**, 1-19. doi:10.3354/meps09831
Ford, J. K. B. and Reeves, R. R. (2008). Fight or flight: antipredator strategies of baleen whales. *Mamm. Rev.* **38**, 50-86. doi:10.1111/j.1365-2907.2008.00118.x
Fournet, M. E., Gabriele, C. M., Sharpe, F., Straley, J. M. and Szabo, A. (2018). Feeding calls produced by solitary humpback whales. *Mar. Mamm. Sci.* **34**, 851-865. doi:10.1111/mms.12485
Friedlaender, A. S., Herbert-Read, J. E., Hazen, E. L., Cade, D. E., Calambokidis, J., Southall, B. L., Stimpert, A. K. and Goldbogen, J. A. (2017). Context-dependent lateralized feeding strategies in blue whales. *Curr. Biol.* **27**, R1193-R1213. doi:10.1016/j.cub.2017.10.023
Friedlaender, A. S., Bowers, M. T., Cade, D., Hazen, E. L., Stimpert, A. K., Allen, A. N., Calambokidis, J., Fahlbusch, J., Segre, P., Visser, F. et al. (2020). The advantages of diving deep: fin whales quadruple their energy intake when targeting deep krill patches. *Funct. Ecol.* **34**, 497-506. doi:10.1111/1365-2435.13471
Glarou, M., Rasmussen, M. H., Poldner, A., Ruppert, S. N. S., Sotiropoulou, D., Sadozai, Z., Jarzynowska, M., Iversen, M. R., Sigurðsson, G. M., Halldórsson, S. D. et al. (2025). Size-specific strategies of sympatric cetaceans to reduce heat loss. *J. Exp. Biol.* **228**, jeb249356. doi:10.1242/jeb.249356
Goldbogen, J. A. and Madsen, P. T. (2018). The evolution of foraging capacity and gigantism in cetaceans. *J. Exp. Biol.* **221**, jeb166033. doi:10.1242/jeb.166033
Goldbogen, J. A., Calambokidis, J., Oleson, E., Potvin, J., Pyenson, N. D., Schorr, G. and Shadwick, R. E. (2011). Mechanics, hydrodynamics and energetics of blue whale lunge feeding: efficiency dependence on krill density. *J. Exp. Biol.* **214**, 131-146. doi:10.1242/jeb.048157
Goldbogen, J. A., Calambokidis, J., Friedlaender, A. S., Francis, J., Deruiter, S. L., Stimpert, A. K., Falcone, E. and Southall, B. L. (2013). Underwater acrobatics by the world's largest predator: 360 rolling manoeuvres by lunge-feeding blue whales. *Biol. Lett.* **9**, 20120986. doi:10.1098/rsbl.2012.0986
Goldbogen, J. A., Hazen, E. L., Friedlaender, A. S., Calambokidis, J., Deruiter, S. L., Stimpert, A. K. and Southall, B. L. (2015). Prey density and distribution drive the three–dimensional foraging strategies of the largest filter feeder. *Funct. Ecol.* **29**, 951-961. doi:10.1111/1365-2435.12395
Goldbogen, J. A., Cade, D. E., Calambokidis, J., Friedlaender, A. S., Potvin, J., Segre, P. S. and Werth, A. J. (2017). How baleen whales feed: the biomechanics of engulfment and filtration. *Ann. Rev. Mar. Sci.* **9**, 367-386. doi:10.1146/annurev-marine-122414-033905
Hain, J. H. W., Carter, G. R., Kraus, S. D., Mayo, C. A. and Winn, H. E. (1982). Feeding behavior of the humpback whale, *Megaptera novaeangliae*, in the Western North Atlantic. *Fish. Bull.* **80**, 259-268.
Hazen, E., Friedlaender, A., Thompson, M., Ware, C., Weinrich, M., Halpin, P. and Wiley, D. (2009). Fine-scale prey aggregations and foraging ecology of humpback whales *Megaptera novaeangliae*. *Mar. Ecol. Prog. Ser.* **395**, 75-89. doi:10.3354/meps08108
Hazen, E. L., Friedlaender, A. S. and Goldbogen, J. A. (2015). Blue whales (*Balaenoptera musculus*) optimize foraging efficiency by balancing oxygen use and energy gain as a function of prey density. *Sci. Adv.* **1**, e1500469. doi:10.1126/sciadv.1500469
Howland, H. C. (1974). Optimal strategies for predator avoidance: the relative importance of speed and manoeuvrability. *J. Theor. Biol.* **47**, 333-350. doi:10.1016/0022-5193(74)90202-1
Jurasz, C. M. and Jurasz, V. P. (1979). Feeding modes of the humpback whale, *Megaptera novaeangliae*, in southeast Alaska. *Sci. Rep. Whales Res. Inst.* **31**, 69-83.
Kahane-Rapport, S. R. and Goldbogen, J. A. (2018). Allometric scaling of morphology and engulfment capacity in rorqual whales. *J. Morphol.* **279**, 1256-1268. doi:10.1002/jmor.20846
Kosma, M. M., Werth, A. J., Szabo, A. R. and Straley, J. M. (2019). Pectoral herding: an innovative tactic for humpback whale foraging. *R. Soc. Open Sci.* **6**, 191104. doi:10.1098/rsos.191104
Kot, B. W., Sears, R., Zbinden, D., Borda, E. and Gordon, M. S. (2014). Rorqual whale (Balaenopteridae) surface lunge–feeding behaviors: standardized classification, repertoire diversity, and evolutionary analyses. *Mar. Mamm. Sci.* **30**, 1335-1357. doi:10.1111/mms.12115
Lockyer, C. (1976). Body weights of some species of large whales. *ICES J. Mar. Sci.* **36**, 259-273. doi:10.1093/icesjms/36.3.259
Long, J. H., Pabst, D. A., Shepherd, W. R. and McLellan, W. A. (1997). Locomotor design of dolphin vertebral columns: bending mechanics and morphology of *Delphinus delphis*. *J. Exp. Biol.* **200**, 65-81. doi:10.1242/jeb.200.1.65
Mastick, N. C. (2016). The effect of group size on individual roles and the potential for cooperation in group bubble-net feeding humpback whales (*Megaptera novaeangliae*). *PhD thesis*, Oregon State University, Corvallis, OR.
Mastick, N. C., Wiley, D., Cade, D. E., Ware, C., Parks, S. E. and Friedlaender, A. S. (2022). The effect of group size on individual behavior of bubble–net feeding

humpback whales in the southern Gulf of Maine. *Mar. Mamm. Sci.* **38**, 959-974. doi:10.1111/mms.12905

McBride, M., Schram Stokke, O., Renner, A., Krafft, B., Bergstad, O., Biuw, M., Lowther, A. and Stiansen, J. (2021). Antarctic krill *Euphausia superba*: spatial distribution, abundance, and management of fisheries in a changing climate. *Mar. Ecol. Prog. Ser.* **668**, 185-214. doi:10.3354/meps13705

McMillan, C. J., Towers, J. R. and Hildering, J. (2019). The innovation and diffusion of "trap–feeding," a novel humpback whale foraging strategy. *Mar. Mamm. Sci.* **35**, 779-796. doi:10.1111/mms.12557

Miklosovic, D. S., Murray, M. M., Howle, L. E. and Fish, F. E. (2004). Leading-edge tubercles delay stall on humpback whale (*Megaptera novaeangliae*) flippers. *Phys. Fluids* **16**, L39. doi:10.1063/1.1688341

Nicol, S., Foster, J. and Kawaguchi, S. (2012). The fishery for Antarctic krill – recent developments. *Fish Fish.* **13**, 30-40. doi:10.1111/j.1467-2979.2011.00406.x

Noren, S. R. and Rosen, D. A. (2023). What are the Metabolic Rates of Marine Mammals and What Factors Impact this Value: A review. *Conserv. Physiol*. **11**, coad077. doi:10.1093/conphys/coad077

Noren, S. R. and Williams, T. M. (2000). Body size and skeletal muscle myoglobin of cetaceans: adaptations for maximizing dive duration. *Comp. Biochem. Physiol. A* **126**, 181-191. doi:10.1016/S1095-6433(00)00182-3

Payne, P. M., Wiley, D. N., Young, S. B., Pittman, S., Clapham, P. J. and Jossi, J. W. (1990). Recent fluctuations in the abundance of baleen whales in the Southern Gulf of Maine in relation to changes in selected prey. *Fish. Bull.* **88**, 687-696.

Pirotta, V., Owen, K., Donnelly, D., Brasier, M. J. and Harcourt, R. (2021). First evidence of bubble–net feeding and the formation of 'super–groups' by the east Australian population of humpback whales during their southward migration. *Aquat. Conserv. Mar. Freshw. Ecosyst.* **31**, 2412-2419. doi:10.1002/aqc.3621

Ryan, C. and Malcolm, A. (2022). Unusual left-handed surface feeding with bubble production in fin whales (*Balaenoptera physalus*). *Aquat. Mamm.* **48**, 517-519. doi:10.1578/AM.48.6.2022.517

Segre, P. S., Cade, D. E., Fish, F. E., Allen, A. N., Calambokidis, J., Friedlander, A. S. and Goldbogen, J. A. (2016). Hydrodynamic properties of fin whale flippers predict rolling performance. *J. Exp. Biol.* **219**, 3315-3320. doi:10.1242/jeb.137091

Segre, P. S., Cade, D. E., Calambokidis, J., Fish, F. E., Friedlaender, A. S., Potvin, J. and Goldbogen, J. A. (2019). Body flexibility enhances maneuverability in the world's largest predator. *Integr. Comp. Biol.* **59**, 48-60. doi:10.1093/icb/icy121

Segre, P. S., Gough, W. T., Roualdes, E. A., Cade, D. E., Czapanskiy, M. F., Fahlbusch, J., Kahane-Rapport, S. R., Oestreich, W. K., Bejder, L., Bierlich, K. C. et al. (2022). Scaling of maneuvering performance in baleen whales: larger whales outperform expectations. *J. Exp. Biol.* **225**, jeb243224. doi:10.1242/jeb.243224

Sharpe, F. A. and Dill, L. M. (1997). The behavior of Pacific herring schools in response to artificial humpback whale bubbles. *Can. J. Zool.* **75**, 725-730. doi:10.1139/z97-093

Snyder, G. K. (1983). Respiratory adaptations in diving mammals. *Respir. Physiol.* **54**, 269-294. doi:10.1016/0034-5687(83)90072-5

Szabo, A., Bejder, L., Warick, H., Van Aswegen, M., Friedlaender, A. S., Goldbogen, J., Kendall-Bar, J. M., Leunissen, E. M., Angot, M. and Gough, W. T. (2024). Solitary humpback whales manufacture bubble-nets as tools to increase prey intake. *R. Soc. Open Sci.* **11**, 240328. doi:10.1098/rsos.240328

van Aswegen, M., Szabo, A., Currie, J. J., Stack, S. H., Straley, J. M., Neilson, J. L., Gabriele, C. M., Baker, C. S., Steel, D., Pack, A. A. et al. (2025). Age-specific body length, mass and energetic cost of growth in humpback whales. *Mar. Ecol Prog Ser.* doi:10.3354/meps14937

Videsen, S. K. A., Simon, M., Christiansen, F., Friedlaender, A., Goldbogen, J., Malte, H., Segre, P., Wang, T., Johnson, M. and Madsen, P. T. (2023). Cheap gulp foraging of a giga-predator enables efficient exploitation of sparse prey. *Sci. Adv.* **9**, eade3889. doi:10.1126/sciadv.ade3889

Visser, I. N., Smith, T. G., Bullock, I. D., Green, G. D., Carlsson, O. G. L. and Imberti, S. (2008). Antarctic peninsula killer whales (*Orcinus orca*) hunt seals and a penguin on floating ice. *Mar. Mamm. Sci.* **24**, 225-234. doi:10.1111/j.1748-7692.2007.00163.x

Watkins, W. A. and Schevill, W. E. (1979). Aerial observation of feeding behavior in four baleen whales: *Eubalaena glacialis*, *Balaenoptera borealis*, *Megaptera novaeangliae* and *Balaenoptera physalus*. *J. Mammal.* **60**, 155-163. doi:10.2307/1379766

Webb, P. W. and De Buffrenil, V. (1990). Locomotion in the biology of large aquatic vertebrates. *Trans. Am. Fish. Soc.* **119**, 629-641. doi:10.1577/1548-8659(1990)119<0629:LITBOL>2.3.CO;2

Weber, P. W., Howle, L. E., Murray, M. M., Reidenberg, J. S. and Fish, F. E. (2014). Hydrodynamic performance of the flippers of large–bodied cetaceans in relation to locomotor ecology. *Mar. Mamm. Sci.* **30**, 413-432. doi:10.1111/mms.12040

Weihs, D. (1993). Stability of aquatic animal locomotion. *Cont. Math.* **141**, 443-461. doi:10.1090/conm/141/19

Weinrich, M. T., Schilling, M. R. and Belt, C. R. (1992). Evidence for acquisition of a novel feeding behaviour: lobtail feeding in humpback whales, *Megaptera novaeangliae*. *Anim. Behav.* **44**, 1059-1072. doi:10.1016/S0003-3472(05)80318-5

Werth, A. J. (2007). Adaptations of the cetacean hyolingual apparatus for aquatic feeding and thermoregulation. *Anat. Rec.* **290**, 546-568. doi:10.1002/ar.20538

Wiley, D., Ware, C., Bocconcelli, A., Cholewiak, D., Friedlaender, A., Thompson, M. and Weinrich, M. (2011). Underwater components of humpback whale bubble-net feeding behaviour. *Behaviour* **148**, 575-602. doi:10.1163/000579511X570893

Woodward, B. L., Winn, J. P. and Fish, F. E. (2006). Morphological specializations of baleen whales associated with hydrodynamic performance and ecological niche. *J. Morphol.* **267**, 1284-1294. doi:10.1002/jmor.10474

Wray, J., Keen, E. and O'Mahony, É. N. (2021). Social survival: humpback whales (*Megaptera novaeangliae*) use social structure to partition ecological niches within proposed critical habitat. *PLoS ONE* **16**, e0245409. doi:10.1371/journal.pone.0245409